

EVALUATION OF BOOMS THEORY

SALAH NOORI ABBOOD

Department of mechanical engineering, College of engineering,
University of Kerbala, Kerbala, Iraq.
jousef_salah@yahoo.ca

ABSTRACT

This paper is concerned with the analysis of closed section beams under bending moments loading. Using theory of booms, five models of circular closed section beams made of eight circular bars and covered with thin plates (of the same material as bars) as a skin where studied under bending moment load to indicate the direct stress at each boom. Finite element method with using ANSYS program was adopted to indicate the direct stresses at the same booms of selected models. A comparison among those types of analysis was made to make an evaluation to booms theory and a correction factor had been suggested to modify this theory.

ملخص البحث

يختص هذا البحث بدراسة العتبات ذات المقاطع المغلقة تحت تأثير عزوم الانحناء. باستخدام نظرية الأعمدة تم دراسة خمسة نماذج من العتبات بمقاطع مغلقة دائرية مشكل كل منها من ثمانية أعمدة دائرية المقطع مغطاة بصفيحة رقيقة الجدران من ذات معدن الأعمدة كغطاء خارجي ومعرضة الى عزم انحناء لتحديد الاجهاد العمودي في كل عمود. كذلك تم استخدام طريقة العناصر المحددة بالاستعانة ببرنامج (ANSYS) الهندسي لتحديد الاجهادات العمودية لذات الأعمدة في النماذج المختارة. تم عمل مقارنة بين نتائج الطريقتين في التحليل لعمل تقييم لنظرية الأعمدة واقتراح معامل تصحيح لتقويم تلك النظرية.

Keywords: booms, closed section beams, idealization.

Nomenclature:

- t_D Shell thickness(mm).
 b Width of the panels(mm).
 B Idealized booms cross-sectional area (mm^2).
 Y Distance between the booms center and sections centroid (mm)
 \bar{Y} Elevation of the centroid (mm)
 \bar{Y} Booms center Elevation (mm).
 A Actual booms cross-sectional area (mm^2).
 R Mean radius of the closed section beam (mm).

1- Introduction:

There are several theories for analyzing stresses and deflections in plates structures These theories can be divided into two major categories: theory for thin plates and theory for thick plates [1].

Booms theory is very efficient method that deals with relatively uncomplicated structural sections. These sections in practice would be formed from thin plate or by the extrusion process. While these sections exist as structural members, they are frequently used to stiffen more complex structural shapes such as fuselages, wings, and closed (or opened) section beams. Thus, a closed section beam could take the form shown in Fig (1-a) in which circular section stringers are used to stiffen the thin skin. The buckling phenomenon in shells is highly complex, described by nonlinear partial differential equations that were too difficult to solve unless some simplifying assumptions were made [2]. Generally, the number and nature of these simplified assumptions determine the accuracy and the degree of complexity of the analysis; the more complex the analysis the greater the accuracy obtained. The degree of introduced simplification is governed by the particular situation surrounding the problem. For a preliminary investigation, speed and simplicity are often of greater importance than extreme accuracy; on the other hand final solution must be as exact as circumstances allows.

Complex structural sections may be idealized into simpler 'mechanical model' forms which behave, under given loading conditions, in a manner similar as possible as the actual structure. Different models of the same structure are required to simulate actual behavior under different systems of loading. In the closed section beam of Fig (1-a), the stringers have small cross sectional dimensions compared with the complete section of the beam. Thus, the variation in stress over the cross-section of a stringer due to, say, bending of the entire beam would be small. Furthermore, the difference between the distances of the stringer centroids and the adjacent skin from the entire beam section axis is small. It would be reasonable to assume therefore that the bending stress is constant over the stringer cross-sections. Thus we could replace the stringers and spar flanges by concentrations of area, known as booms, over which the direct stress is constant and which are located along the mid-line of the skin, as shown in Fig (1-b).

2- Theory of booms:

In stiffened closed shell with circular sections (Fig. 1-a), the stringers carry most of the bending stresses while the skin is mainly effective in resisting shear stresses although it also carries some of the direct stresses. Transverse shear deformation effects are important in determining maximum deflections, vibration natural frequency, and critical buckling loads [3]. Fig (2) shows the idealization of these types of section beams. It may therefore be taken a stage further by assuming that all direct stresses are carried by the booms while the skin is effective only in shear.

The allowable bending stress capacity of the skin is obtained by increasing each boom area with an area equivalent to the direct stress carrying capacity of the adjacent skin panels. The calculation of these equivalent areas will generally depend upon an initial assumption as to the form of the distribution of direct stress in a boom/skin panel.

To idealize the panel of Fig (2-a) into a combination of booms carrying bending stress and skin carrying only shear stress as shown in Fig (1-b), we suppose that the direct stress carrying thickness (t_D) of the skin is equal to its actual thickness (t) while in Fig (2-b) $t_D = 0$ [4]. Suppose also that the direct stress distribution in the actual panel varies linearly from an unknown value (σ_1) to an unknown value (σ_2). Clearly the analysis should predict the extremes of stress (σ_1) and (σ_2) although the distribution of direct stress is obviously lost. Since the loading producing the direct stresses in the actual and idealized panels must be the same we can equate moments to obtain expressions for the boom areas (B_1) and (B_2). Thus, taking moments about point C:

$$\sigma_2 t_D \frac{b^2}{2} + \frac{1}{2} (\sigma_1 - \sigma_2) t_D b \frac{2}{3} b = \sigma_1 B_1 b$$

Whence

$$B_1 = \frac{t_D b}{6} \left(2 + \frac{\sigma_2}{\sigma_1} \right) \dots\dots\dots (1)$$

Similarly,

$$B_2 = \frac{t_D b}{6} \left(2 + \frac{\sigma_1}{\sigma_2} \right) \dots\dots\dots (2)$$

In Equations (1) and (2) the ratio of (σ_1) to (σ_2), if not known, may frequently be assumed.

The stresses ratio ($\sigma_1/\sigma_2 = -1$) and ($B_1 = B_2 = t_D b/6$) since the stress distribution in Fig (2-a) is caused by a pure bending moment [4].

The bending stress for each boom will be calculated using the following equation:

$$\sigma_z = \frac{M_x}{\sum I_{xx}} Y \dots\dots\dots (3)$$

3- Mathematical models:

To evaluate theory of booms, five models were selected. They are a circular closed section beam shown in Fig (1-a) with mean diameter of (500 mm) built from eight circular bars with cross-sectional areas illustrated in (table-1) and skin thicknesses of (1, 1.5, 2, 2.5, 3) mm respectively.

All models are subjected to bending moment of (20kN.m). That means fixing all parameter except skin thickness to evaluate the ability of theory of booms to deal with this important parameter (i.e. that we can use any numerical values for the above parameters for this purpose). Ansys programme is used also to calculate stresses in sections of them as shown in Fig (3) which represents a simulation of circular closed section beam with skin thickness of (1mm) and parameters listed in (table-1). Similarly other models were simulated and there results were obtained.

4- Calculations:

Equations (1) and (2) will be rewritten for our models as follows:

$$B_i = A_i + \left[\frac{t_D \times b}{6} \left(2 + \frac{\sigma_{i-1}}{\sigma_i} \right) \right] + \left[\frac{t_D \times b}{6} \left(2 + \frac{\sigma_{i+1}}{\sigma_i} \right) \right] \dots\dots\dots (4)$$

For beams,

$$\frac{\sigma_{i-1}}{\sigma_i} = \frac{Y_{i-1}}{Y_i} \quad \text{And} \quad \frac{\sigma_{i+1}}{\sigma_i} = \frac{Y_{i+1}}{Y_i}$$

So equation will take the following form:

$$B_i = A_i + \left[\frac{t_D \times b}{6} \left(2 + \frac{Y_{i-1}}{Y_i} \right) \right] + \left[\frac{t_D \times b}{6} \left(2 + \frac{Y_{i+1}}{Y_i} \right) \right] \dots\dots\dots (5)$$

For the first boom, ($Y_{i-1} = Y_8$) and for the last boom, ($Y_{i+1} = Y_1$).

To locate center of gravity for models we use following equation:

$$\sum A_i \bar{\bar{Y}}_i = \bar{\bar{Y}} \sum A_i \quad (I = 1 \text{ to } 8) \quad \dots\dots\dots (6)$$

The length of skin between any two booms is the length of arc with angle of $\left(\frac{\pi}{4}\right)$.

From Fig (1-b), $Y = \bar{\bar{Y}} - \bar{Y}$.

5- Results and discussion:

The angle separates booms of any models is $\left(\frac{\pi}{4}\right)$. By using ($R= 250\text{mm}$) and from Fig (1-b) we obtained:

$$\begin{aligned} \bar{\bar{Y}}_5 &= 0 \quad \text{And} \quad \bar{\bar{Y}}_1 = 500\text{mm} \\ \bar{\bar{Y}}_3 &= \bar{\bar{Y}}_7 = R = 250\text{mm} \\ \bar{\bar{Y}}_2 &= \bar{\bar{Y}}_8 = R \left(1 + \cos \frac{\pi}{4} \right) = 426.78\text{mm} \\ \bar{\bar{Y}}_4 &= \bar{\bar{Y}}_6 = R \left(1 - \cos \frac{\pi}{4} \right) = 73.223\text{mm} \end{aligned}$$

Applying equation (6) on all models with parameters of (table-1) and Fig (1) gives

$$\bar{Y} = 266.13mm$$

So, (Y) will be positive for booms (1, 2, and 8) and will be negative for booms (3, 4, 5, 6, and 7) as shown in (table-2).

With the use of equations (5) and (3) for $(b = \frac{\pi R}{4} = \frac{\pi(250)}{4} = 196.35mm)$ we concluded the direct stresses of all booms of different models as shown in tables (3 to 7).

To indicate direct stresses in booms of the selected models using finite elements method with the help of Ansys program, critical areas where loads or stresses are concentrated will generally be need to finer element mesh [5]. Thus, all models were divided into elements with edge length of (5 mm) as shown in Fig (3). This edge length is the minimum value to satisfy acceptable results Fig (4). Tables (3 to 7) illustrate stresses results for all models.

The average of ratios of direct stresses obtained using Ansys program and those obtained by theory of booms are as follows:

| | | | | | |
|----------------------|--------|--------|--------|--------|--------|
| Shell thickness (mm) | 1 | 1.5 | 2 | 2.5 | 3 |
| Stresses ratio | 0.9542 | 0.9552 | 0.9565 | 0.9573 | 0.9567 |

We note as a general that an increasing in the shell thickness leads to an increasing in stresses ratio. That was because of behavior of tested closed section beams under loading as shown in Fig (5). This behavior is more significant with use of thinner shells.

6- Conclusions:

- 1.Theory of booms is the simpler method to deal with closed section beams that fabricated from a number of booms covered with an external plate as a skin.
- 2.This theory has not a perfect accuracy but can be used directly with a convenient safety factor.
- 3.For more accuracy and as an average, the general stress ratio found as (0.956) and this ratio can be used as a correction factor to evaluate booms theory with any thickness of skin.

References

- [1] Liu G.R., "Mesh Free Methods", CRC Press LLC, 2003, page 40.
- [2] Teng J.G. and Rotter J.M., "Buckling of Thin Metal Shells", First Edition, Spon Press, 2005, Page 7.
- [3] Gladwell G.M.L., "Solid Mechanics and Its Applications Series", Volume120, Springer, 2005, Page 209.
- [4] Megson T.H.G., "Aircraft Structures", Third Edition, John Wiley, 1999, Page 327-331.
- [5] Yong Bai, "Marine Structural design", First Edition, Elsevier, 2003, Page 106.

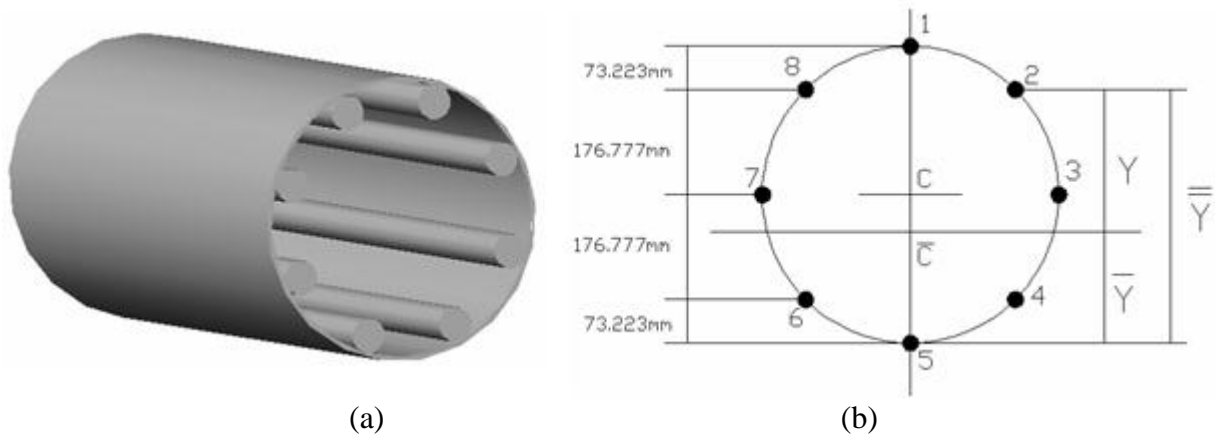


Fig (1) Closed section beam under bending loading and its idealization

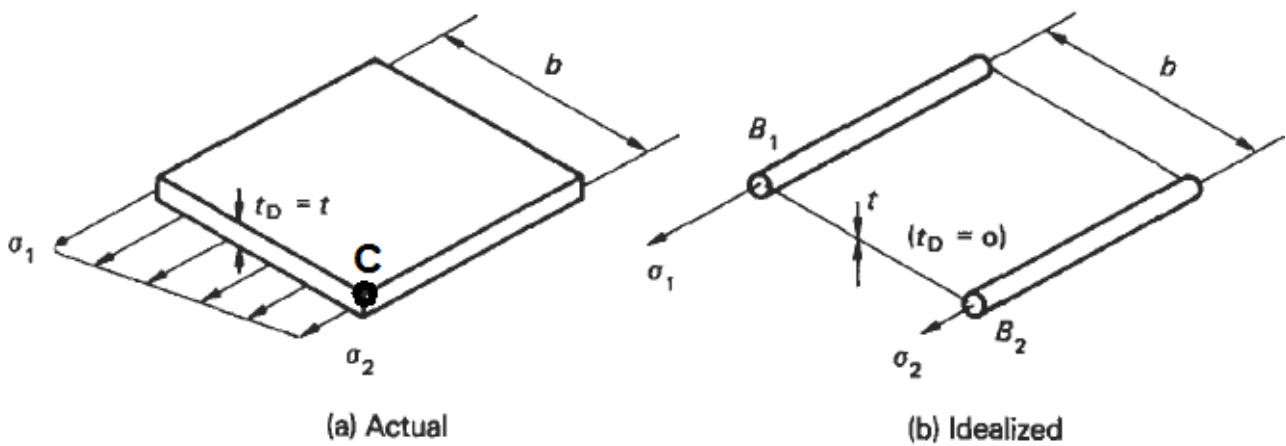


Fig (2) panels Idealization.

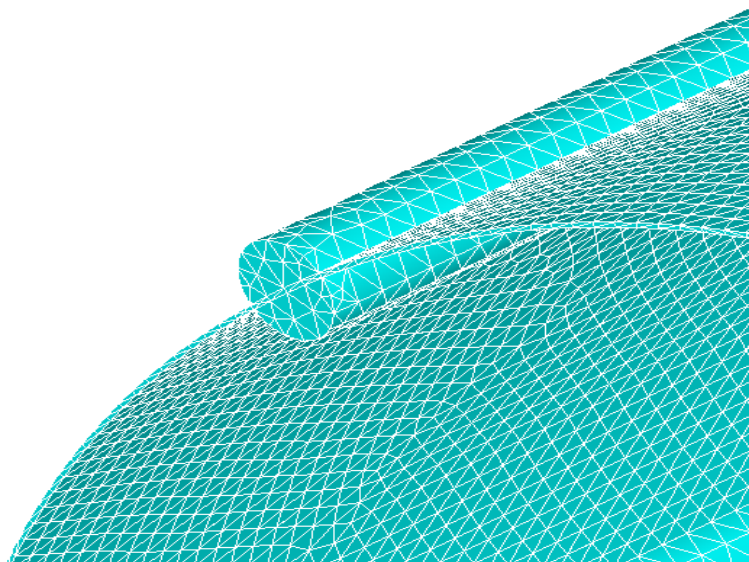


Fig (3) elements divisions using Ansys program

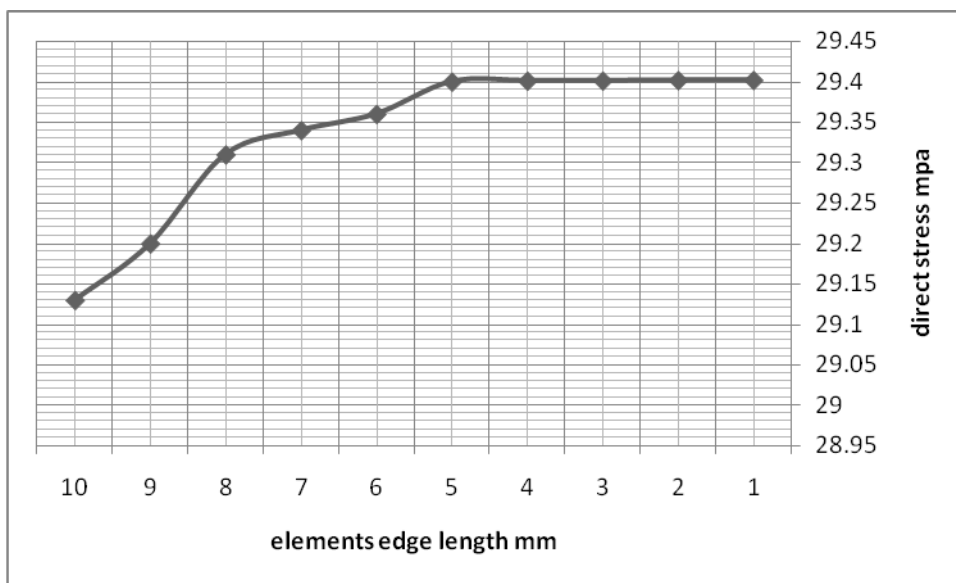


Fig (4) divergence of stresses in boom No.1 for (1mm shell thickness)

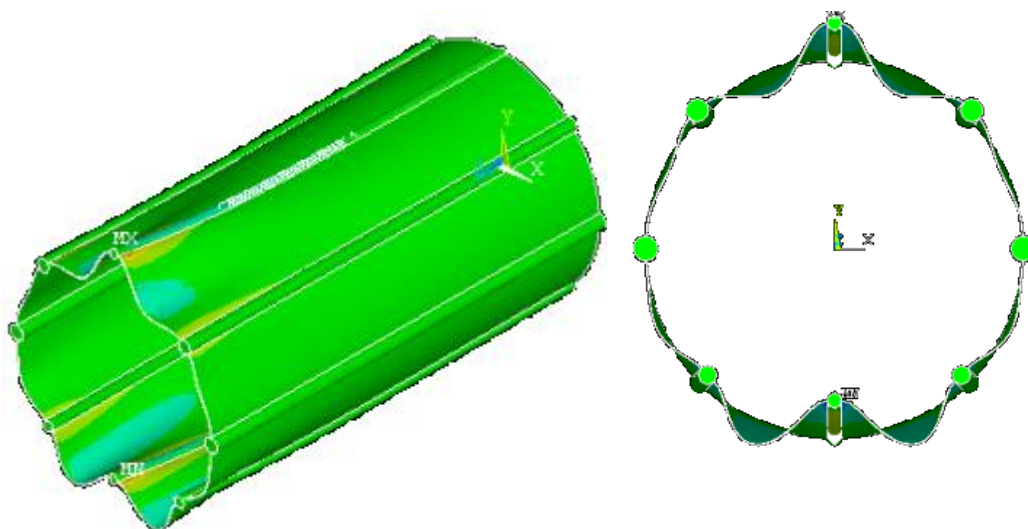


Fig (5) Behavior of tested closed section beams under bending loading

(Table-1) Areas for booms of closed section models

| Boom | 1 | 2 | 3 | 4 | 5 | 6 | 7 | 8 |
|-------------------------|--------|--------|-------|--------|--------|--------|-------|--------|
| Diameter (mm) | 20 | 30 | 33 | 25 | 20 | 25 | 33 | 30 |
| Area (mm ²) | 314.16 | 706.86 | 855.3 | 490.87 | 314.16 | 490.87 | 855.3 | 706.86 |

(Table-2) Distribution of booms

| Boom | 1 | 2 | 3 | 4 | 5 | 6 | 7 | 8 |
|----------------|--------|--------|--------|----------|---------|----------|--------|--------|
| Y (mm) | 233.87 | 160.65 | -16.13 | -192.907 | -266.13 | -192.907 | -16.13 | 160.65 |
| \bar{Y} (mm) | 500 | 426.78 | 250 | 73.223 | 0 | 73.223 | 250 | 426.78 |

(Table-3) Results for a model with skin thickness of (1mm)

| Boom | 1 | 2 | 3 | 4 | 5 | 6 | 7 | 8 |
|--|--------------|----------------|---------------|---------------|---------------|---------------|---------------|----------------|
| B (mm ²) | 490.02 | 882.11 | 1051.644 | 669.653 | 492.5 | 669.653 | 1051.644 | 882.11 |
| I _{xx} =BY ² (mm ⁴) | 26.8 E+06 | 22.766 E+06 | 0.274 E+06 | 24.92 E+06 | 34.88 E+06 | 24.92 E+06 | 0.274 E+06 | 22.766 E+06 |
| σ _z (N/mm ²) | 29.7 | 20.4 | -2.05 | -24.5 | -33.8 | -24.5 | -2.05 | 20.4 |
| σ _z (N/mm ²) (using ANSYS) | 29.4 | 20.101 | -1.7493 | -24.198 | -33.5 | -24.198 | -1.7493 | 20.101 |

(Table-4) Results for a model with skin thickness of (1.5mm)

| Boom | 1 | 2 | 3 | 4 | 5 | 6 | 7 | 8 |
|--|---------------|---------------|-------------|---------------|--------------|---------------|-------------|---------------|
| B (mm ²) | 577.95 | 969.742 | 1149.816 | 759.04 | 581.673 | 759.04 | 1149.816 | 969.742 |
| I _{xx} =BY ² (mm ⁴) | 31.61 E+06 | 25.03 E+06 | 0.3 E+06 | 28.25 E+06 | 41.2 E+06 | 28.25 E+06 | 0.3 E+06 | 25.03 E+06 |
| σ _z (N/mm ²) | 26 | 17.853 | -1.79 | -21.44 | -29.575 | -21.44 | -1.79 | 17.853 |
| σ _z (N/mm ²) (using ANSYS) | 25.739 | 17.601 | -1.532 | -21.19 | -29.316 | -21.19 | -1.532 | 17.601 |

(Table-5) Results for a model with skin thickness of (2mm)

| Boom | 1 | 2 | 3 | 4 | 5 | 6 | 7 | 8 |
|--|---------------|---------------|---------------|---------------|--------------|---------------|---------------|---------------|
| B (mm ²) | 665.88 | 1057.37 | 1248 | 848.436 | 670.844 | 848.436 | 1248 | 1057.37 |
| I _{xx} =BY ² (mm ⁴) | 36.42 E+06 | 27.29 E+06 | 0.325 E+06 | 31.57 E+06 | 47.5 E+06 | 31.57 E+06 | 0.325 E+06 | 27.29 E+06 |
| σ _z (N/mm ²) | 23.12 | 15.882 | -1.595 | -19.07 | -26.31 | -19.07 | - 1.595 | 15.882 |
| σ _z (N/mm ²) (using ANSYS) | 22.87 | 15.671 | -1.372 | -18.847 | -26.101 | -18.847 | - 1.372 | 15.671 |

(Table-6) Results for a model with skin thickness of (2.5mm)

| Boom | 1 | 2 | 3 | 4 | 5 | 6 | 7 | 8 |
|--|---------------|---------------|--------------|--------------|---------------|--------------|--------------|---------------|
| B (mm ²) | 753.8 | 1145 | 1346.16 | 937.83 | 760 | 937.83 | 1346.16 | 1145 |
| I _{xx} =BY ² (mm ⁴) | 41.23 E+06 | 29.55 E+06 | 0.35 E+06 | 34.9 E+06 | 53.83 E+06 | 34.9 E+06 | 0.35 E+06 | 29.55 E+06 |
| σ _z (N/mm ²) | 20.82 | 14.3 | -1.436 | -17.17 | -23.7 | -17.17 | -1.436 | 14.3 |
| σ _z (N/mm ²) (using ANSYS) | 20.613 | 14.121 | -1.237 | -17 | -23.48 | -17 | -1.237 | 14.121 |

(Table-7) Results for a model with skin thickness of (3mm)

| Boom | 1 | 2 | 3 | 4 | 5 | 6 | 7 | 8 |
|--|---------------|--------------|---------------|---------------|---------------|---------------|---------------|--------------|
| B (mm ²) | 841.74 | 1232.62 | 1444.33 | 1027.22 | 849.19 | 1027.22 | 1444.33 | 1232.62 |
| I _{xx} =BY ² (mm ⁴) | 46.04 E+06 | 31.8 E+06 | 0.376 E+06 | 38.23 E+06 | 60.14 E+06 | 38.23 E+06 | 0.376 E+06 | 31.8 E+06 |
| σ _z (N/mm ²) | 18.937 | 13 | -1.306 | -15.62 | -21.55 | -15.62 | -1.306 | 13 |
| σ _z (N/mm ²) (using ANSYS) | 18.76 | 12.802 | -1.1256 | -15.45 | -21.37 | -15.45 | -1.1256 | 12.802 |